The Hyperfine Structure and Nuclear Moments of the Stable Chlorine Isotopes*

LUTHER DAVIS, JR., BERNARD T. FELD, CARROL W. ZABEL,** AND JERROLD R. ZACHARIAS
*Department of Physics and Research Laboratory of Electronics, Massachusetts Institute of Technology,*** Cambridge, Massachusetts*
(Received July 12, 1949)

The hyperfine structure of the $^2P_{3/2}$ ground states of Cl^{35} and Cl^{37} is investigated by the atomic beam magnetic resonance method. Values of the magnetic dipole interaction constant, a, and the electric quadrupole interaction constant, b, are found to be

$$a_{35}=205.288\pm0.010 \text{ Mc/sec.}, \quad a_{37}=170.686\pm0.010 \text{ Mc/sec.},$$
$$b_{35}=55.347\pm0.020 \text{ Mc/sec.}, \quad b_{37}=43.256\pm0.020 \text{ Mc/sec.}$$

No octupole interaction is required to account for the experimental results. A simple method is introduced for calculating accurate values of the electric quadrupole moments Q from these data and the corresponding values are

$$Q_{35}=-(0.0795\pm0.0005)\times10^{-24} \text{ cm}^2 \quad \text{and} \quad Q_{37}=-(0.0621\pm0.0005)\times10^{-24} \text{ cm}^2.$$

This method can be extended to many other cases for which the interaction constants a and b and the nuclear gyromagnetic ratio are known. Experimental details are given for the production and detection of beams of atomic chlorine.

I. INTRODUCTION

IN the preceding paper, henceforth referred to as DNZ, an atomic beam detecting system, capable of the separate identification of individual isotopes, has been described. In the course of those experiments it was found that a beam of chlorine could be detected. Chlorine atoms, when allowed to fall on a hot tungsten ribbon, evaporate as negative ions. These are separated, by the mass spectrometer, from the electrons which are emitted by the tungsten, and are measured as a negative ion current by an electrometer.

Chlorine contains two stable isotopes of mass numbers 35 and 37 and abundances of 75 percent and 25 percent, respectively. The nuclei of both isotopes are known[1] to have spins of 3/2. The nuclear moments were measured by Kusch and Millman[2] and by Bitter.[3] Taub and Kusch[4] have recently re-evaluated the moments; they give for the magnetic moments in nuclear magneton units:

$$\mu^{35}=+0.8222\pm0.032 \text{ percent};$$
$$\mu^{37}=+0.683\pm0.44 \text{ percent}.$$

Hyperfine structure has been observed, by the technique of microwave spectroscopy, in transitions between rotational levels in a variety of molecules containing chlorine.[1,5] The structure has been attributed to an electrostatic interaction between the nuclear electric quadrupole moment and the gradient of the molecular electric field at the chlorine nucleus. The "quadrupole coupling," eQd^2V/dz^2, has been observed for the chlorine nuclei in the simple polyatomic molecules, ClCN, ICl, and CH_3Cl.

Townes[6] has outlined a procedure for estimating d^2V/dz^2 in some molecules, based on arguments which indicate that for molecules in which Cl is covalently bonded, the gradient of the electric field at the Cl nucleus is only slightly different from the gradient in the Cl atom in the ground state. On this basis, Townes estimated the nuclear electric quadrupole moments of the Cl isotopes to be

$$Q^{35}=-6.7\times10^{-26} \text{ cm}^2;$$
$$Q^{37}=-5.1\times10^{-26} \text{ cm}^2.$$

The possibility of detecting a beam of atomic chlorine makes it feasible to measure the hyperfine structure splitting in the ground state of atomic chlorine, by the atomic beam magnetic resonance method.[7] Since the ground state of Cl is a $^2P_{3/2}$ configuration, a measurement of the hyperfine structure splitting allows a direct evaluation of the nuclear electric quadrupole moment, as described in the following section.

II. THEORY

In the present paper we are presenting the theory of atomic hyperfine structure and its Zeeman effect in greater detail than has been done by other investigators.[8,9] In applying the radiofrequency methods to atomic spectra it is frequently difficult to find some of the spectral lines necessary for the evaluation of the constants. It is also a complicated process to make a positive identification of the lines, when found. The experimental procedures lean heavily on theory because, if the interaction constants are not known in advance,

* Preliminary results have been reported in Phys. Rev. 73, 525 (1948).
** Now at Los Alamos Scientific Laboratory, Los Alamos, New Mexico.
*** This work has been supported in part by the Signal Corps, the Air Materiel Command, and the ONR.
[1] Townes, Holden, Bardeen, and Merritt, Phys. Rev. 71, 644 (1947).
[2] P. Kusch and S. Millman, Phys. Rev. 56, 527 (1939).
[3] F. Bitter, Phys. Rev. 75, 1326 (1949).
[4] H. Taub and P. Kusch, Phys. Rev. 75, 1481 (1949).
[5] Gordy, Simmons, and Smith, Phys. Rev. 72, 344 (1947).
[6] C. H. Townes, Phys. Rev. 71, 909 (1947).
[7] Kusch, Millman, and Rabi, Phys. Rev. 57, 765 (1940).
[8] D. R. Hamilton, Phys. Rev. 56, 30 (1939).
[9] N. A. Renzetti, Phys. Rev. 57, 753 (1940); G. E. Becker and P. Kusch, Phys. Rev. 73, 584 (1948).

it is necessary to use methods of successive approximation, which are alternatively theoretical and experimental, in order to determine where in the radiofrequency spectrum to search. Since a new method is presented for making accurate evaluations of nuclear quadrupole moments, it seems profitable to clarify the nature of the assumptions on which it is based.

A. The Hyperfine Structure Pattern in a Magnetic Field

The hyperfine structure of the ground state of chlorine arises out of two effects. The first is the magnetic dipole-dipole interaction, resulting from the interaction between the nuclear magnetic dipole moment with the magnetic field, at the position of the nucleus, due to the electronic configuration; the hyperfine splitting resulting from this interaction obeys the "interval rule." The second interaction is due to the nuclear electric quadrupole moment; it gives rise to deviations from the interval rule.

Characterizing the atomic electron configuration by the total angular momentum quantum number, J, and the nucleus by the spin I, the terms in the Hamiltonian for the atom which lead to the hyperfine splitting are conveniently[a] written:[10]

$$(1/h)\mathcal{H}(\text{h.f.s.})=a\mathbf{I}\cdot\mathbf{J}+bQ_{\text{op}}, \tag{1}$$

where

$$Q_{\text{op}}=\frac{3(\mathbf{I}\cdot\mathbf{J})^2+(3/2)(\mathbf{I}\cdot\mathbf{J})-I(I+1)J(J+1)}{2I(2I-1)J(2J-1)}, \tag{2}$$

and a and b are constants, of dimensions sec.$^{-1}$, characterizing the atomic and nuclear magnetic and electric properties. $Q_{\text{op}}=0$ for $J=0$ or $\frac{1}{2}$. Both terms are diagonal in the representation in which $\mathbf{F}=\mathbf{I}+\mathbf{J}$ and $m=F_z$ are good quantum numbers. For the ground state of chlorine, $I=J=\frac{3}{2}$, the relative positions of the h.f.s. levels, with respect to their center of gravity, are

$$\begin{aligned}(E/ha)_{F=0}&=-15/4+5\gamma/4,\\ (E/ha)_{F=1}&=-11/4+\gamma/4,\\ (E/ha)_{F=2}&=-\tfrac{3}{4}-\tfrac{3}{4}\gamma,\\ (E/ha)_{F=3}&=9/4+\gamma/4,\end{aligned} \tag{3}$$

where $\gamma=b/a$.

The application of an external (constant) magnetic field H, along the z axis, will remove the degeneracy. If the magnetic field is of such strength that the magnetic interaction energy is *small* compared to the *fine* structure splitting, but not necessarily small compared to the hyperfine structure splitting, the Hamiltonian becomes

$$\mathcal{H}=\mathcal{H}(\text{h.f.s.})+\mathcal{H}(\text{mag}), \tag{4}$$

$$\mathcal{H}(\text{mag})=\mu_0(g_J\mathbf{J}\cdot\mathbf{H}+g_I\mathbf{I}\cdot\mathbf{H}). \tag{5}$$

In the above $\mu_0=e\hbar/2mc$, the Bohr magneton; g_J is the Landé g-factor for the electronic configuration, and g_I is the nuclear g-factor. It is convenient to express $\mathcal{H}(\text{mag})$ in the following form:

$$\mathcal{H}'(\text{mag})=\mathcal{H}(\text{mag})/ha=xJ_z+(g_I/g_J)xI_z, \tag{6}$$

where[b] $x=\mu_0 g_J H/ha$.

The matrix for $\mathcal{H}(\text{mag})$, in the F, m representation, contains off-diagonal elements connecting terms of the same m but with F differing by ±1. The required matrix elements are given by Condon and Shortley,[11] they are

$$(F,m|J_z|F+1,m)=-\left\{\frac{[(F+1)^2-(J-I)^2](I+J+2+F)(I+J-F)[(F+1)^2-m^2]}{4(F+1)^2(2F+1)(2F+3)}\right\}^{\frac{1}{2}}, \tag{7}$$

$$(F,m|J_z|F,m)=\left\{\frac{F(F+1)+J(J+1)-I(I+1)}{2F(F+1)}\right\}\text{or,} \tag{8}$$

$$(F,m|J_z|F-1,m)=-\left\{\frac{[F^2-(J-I)^2][(I+J+1)^2-F^2][F^2-m^2]}{4F^2(4F^2-1)}\right\}^{\frac{1}{2}}. \tag{9}$$

The matrix elements for I_z are obtained by interchanging I and J when $\Delta F=0$, and by multiplying by -1 when $\Delta F=\pm1$, in the above relations.

The energy values of the system in an external magnetic field can now be obtained by solving the secular equation derived from the matrix $\mathcal{H}$. The secular equation factors into one fourth-order determinant and pairs of first-order, second-order and third-order determinants. The determinantal equations have been evaluated numerically for various values of x and γ, assuming $g_I=0$ (i.e., neglecting the term in (g_I/g_J)). The results are being collected, to be issued in a technical report of the M.I.T. Research Laboratory of Electronics. The results, for $\gamma=0$, are plotted in Fig. 1, where E/ha is plotted against x (proportional to the external magnetic field).

[a] Our definition of b differs from the one frequently used in spectroscopy, according to which the quadrupole term is taken to be $bC(C+1)$.

[10] H. Kopferman, *Kernmomente* (Edwards Brothers, Inc., Ann Arbor, Michigan, 1945).

[b] This definition of x is slightly different from the one conventionally used in cases when $J=1/2$. Becker and Kusch (see reference 9) use the same definition in their interpretation of the $^2P_{3/2}$ state of Ga.

[11] E. U. Condon and G. H. Shortley, *Theory of Atomic Spectra*, (Cambridge University Press, London, 1935), pp. 63, 64, and 67.

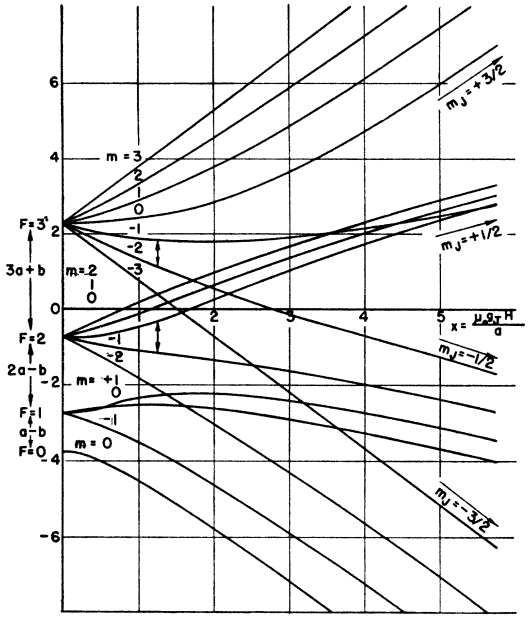

FIG. 1. Diagram to show dependence on magnetic field of the energy levels of an atom with nuclear angular momentum $I=3/2$ and electronic angular momentum $J=3/2$ on the assumption that the electron nuclear interaction arises only from magnetic dipole coupling.

B. Selection Rules and Transition Probabilities

In the magnetic resonance method, as employed in these experiments, transitions between the h.f.s. energy levels are induced by the application of a relatively weak, oscillating magnetic field. The effect of the oscillating field can be described by adding to the Hamiltonian of the system a perturbation of the form

$$\mathcal{H}'=\mu_0(g_J\mathbf{J}+g_I\mathbf{I})\cdot\mathbf{H}', \tag{10}$$

where

$$H'=(H_x'\mathbf{i}+H_y'\mathbf{j}+H_z'\mathbf{k})\sin\omega t. \tag{11}$$

In the Zeeman region of the h.f.s. the possible transitions are those for which there exist non-vanishing matrix elements of $\mathcal{H}'$ in the F, m representation.[11] These are easily seen to obey the conditions $\Delta F=0$, ±1, $\Delta m=0$, ±1. The matrix elements for $m=0$ are proportional to H_z', while those of $\Delta m=\pm1$ are proportional to $(H_x'+iH_y')$. In the experiments herein reported, the oscillating field has components in all three directions, thereby permitting the observation of both types of transitions.

Of particular interest is the value of the transition probability at resonance. It can be shown[12] that, provided the transition probability, $P_{Fm;F'm'}$, is small compared to one,

$$h^2P_{Fm;F'm'}\cong\pi^2t^2\mu_0^2g_J^2 \times|(F,m|J_xH_x'+J_yH_y'+J_zH_z'|F',m')|^2, \tag{12a}$$

where t is the time spent by the atom in the oscillating magnetic field. Because of the different values of the transition matrix element for different transitions, as seen in Table I, the optimum oscillating fields may differ by an order of magnitude from transition to transition.

C. Nuclear Moments from the Hyperfine Structure

In the absence of externally applied fields, the hyperfine structure interaction Hamiltonian is diagonal in the F, m representation; the positions of the h.f.s. levels (in units of sec.$^{-1}$) are

$$(E/h)_F=\frac{aC}{2}+b\left\{\frac{\frac{3}{4}C(C+1)-I(I+1)J(J+1)}{2I(2I-1)J(2J-1)}\right\}, \tag{12b}$$

where $C=F(F+1)-I(I+1)-J(J+1)$. Thus, measurement of the frequency difference between the h.f.s.

TABLE I. $|(F,m|\mathbf{J}|F';m')|^2\times40$ for $I=J=3/2$. The bold numbers correspond to $\Delta m=0$; these must be multiplied by $H'_z{}^2$ to obtain the required matrix element factor in the transition probability. The others must be multiplied by $(H'_x{}^2+H'_y{}^2)$.

F', m' \ F,m	3, 3	3, 2	2, 2	3, 1	2, 1	1, 1	3, 0	2, 0	1, 0	0, 0	1, −1	2, −1	3, −1	2, −2	3, −2	3, −3
3, 3	—	15	15													
3, 2	15	—	**10**	25	10											
2, 2	15	**10**	—	1	10	24*										
3, 1		25	1	—	**16**		30	6								
2, 1		10	10	**16**	—	24*	3	15	12*							
1, 1			24*		24*	—		4*	5	25						
3, 0				30	3		—	**18**				3†	30			
2, 0				6	15	4*	**18**	—	**32***		4	15*	6			
1, 0					12*	5		**32***	—	**50**	5	12				
0, 0						25			**50‡**	—	25					
1, −1								4†	5	25	—	24		24		
2, −1							3	15*	12		24	—	16*	10	10	
3, −1							30	6				16*	—	1	25*	
2, −2											24	10	1†	—	**10**	15
3, −2												10	25*	**10**	—	15
3, −3														15	15	—

* Observable in our experiment by the ordinary refocusing condition.
† Observable in our experiment by the special refocusing condition.
‡ Transition used to obtain the $F=1$, $F=0$ energy difference.

[12] I. I. Rabi, Phys. Rev. **51**, 652 (1937).

lines, in zero magnetic field, leads directly to the determination of a and b.

The evaluation of the nuclear moments from the constants a and b has been discussed in complete detail by Casimir.[13] In the following, we abstract those of his results which are applicable to the experiments discussed in this and the following paper.

For an atom in which there is a single valence electron, in addition to any number of completed shells, the wave function for the valence electron can usually be written as a product of a spacial term, a term involving the orbital angular momentum (spherical harmonic), and a spin term. The magnetic h.f.s. constant, a, arises from the interaction between the nuclear magnetic dipole moment and the magnetic field, at the position of the nucleus, due to the electronic configuration

$$E_{\text{mag}} = -\boldsymbol{\mu}_{\text{nucl}} \cdot \mathbf{H}_{\text{elect}}.$$

The magnetic field at the nucleus is

$$\mathbf{H}_{\text{elect}} = -\mu_0 \langle r^{-3} \rangle_{\text{Av}} f(L, J) \mathbf{J},$$

which, when combined with

$$\boldsymbol{\mu}_{\text{nucl}} = -\mu_0 g_I \mathbf{I},$$

yields

$$ha = E_{\text{mag}}/(\mathbf{I} \cdot \mathbf{J}) = -\mu_0^2 g_I \langle r^{-3} \rangle_{\text{Av}} f(L, J). \quad (13)$$

In the above $\langle r^{-3} \rangle_{\text{Av}}$ is obtained by averaging over the spacial part of the electron wave function, and

$$f(L, J) = \frac{2L(L+1)}{J(J+1)} \mathfrak{F}, \text{ for } J = L \pm 1/2;$$

$\mathfrak{F}$ is a small relativistic correction, given by Casimir.[13]

The electric quadrupole interaction energy is given the expression

$$hb = E_{\text{quad}} = -e^2 Q \left\langle \left\{ \frac{3\cos^2\theta - 1}{r^3} \right\}_{J,J} \right\rangle_{\text{Av}}, \quad (14)$$

where the subscripts indicate that the average is to be taken over the electronic configuration in the state $m_J = J$. The nuclear electric quadrupole moment is conventionally defined as

$$Q = Z\langle (3z^2 - r^2)_{I,I} \rangle_{\text{Av}}, \text{ averaged over the nucleus.}$$

On the assumption of the separability of the electron wave function,

$$\left\langle \left\{ \frac{3\cos^2\theta - 1}{r^3} \right\}_{J,J} \right\rangle_{\text{Av}} = \langle (r^{-3}) \rangle_{\text{Av}} R \langle (3\cos^2\theta - 1)_{J,J} \rangle_{\text{Av}}, \quad (15)$$

[13] H. B. G. Casimir, *On the Interaction between Atomic Nuclei and Electrons* (Teyler's Tweede Genootschap, Haarlem, 1936), pp. 57, 58.

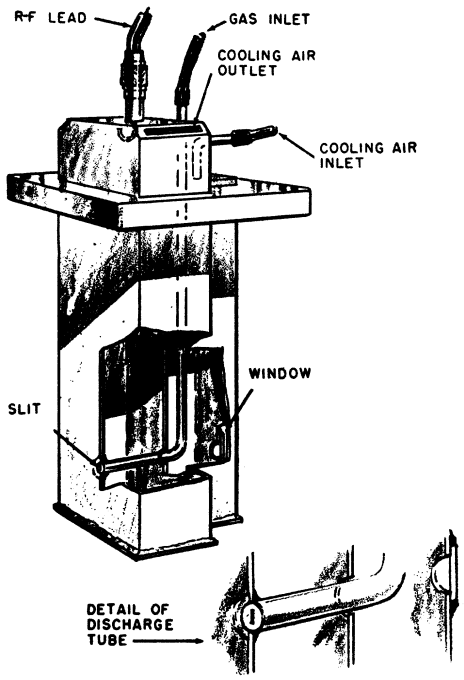

FIG. 2. Cut-away sketch of resonant cavity and gas system for producing atomic chlorine from Cl_2.

with

$$\langle (3\cos^2\theta - 1)_{J,J} \rangle_{\text{Av}} = \frac{-2L}{2L+3} \text{ for } J = L + 1/2. \quad (16)$$

R is still another small relativistic correction. For other values of $J \neq L + \frac{1}{2}$ the evaluation of $\langle (3\cos^2\theta - 1)_{J,J} \rangle_{\text{Av}}$ is somewhat more complicated, but we need only point out that

$$\langle (3\cos^2\theta - 1)_{J,J} \rangle_{\text{Av}} = 0 \text{ for } J = \tfrac{1}{2}.$$

In the particular case of interest in our experiments, the electronic configuration is $^2P_{3/2}$. It is, however, important to note that for chlorine, we are dealing not with a single valence electron, but with an electron shell which lacks a single electron of being closed. As

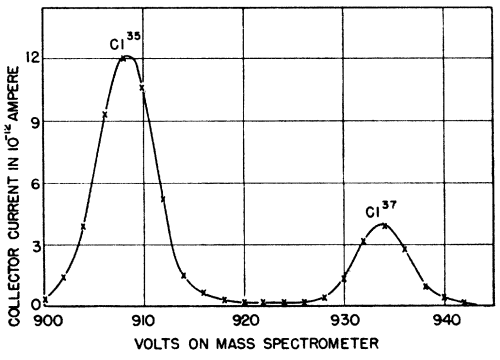

FIG. 3. Mass spectrometer curve presented to show ease with which it is possible to work with the separate chlorine isotopes. Care must be taken to avoid searching for Cl^{37} spectrum lines with the mass spectrograph set for mass 35.

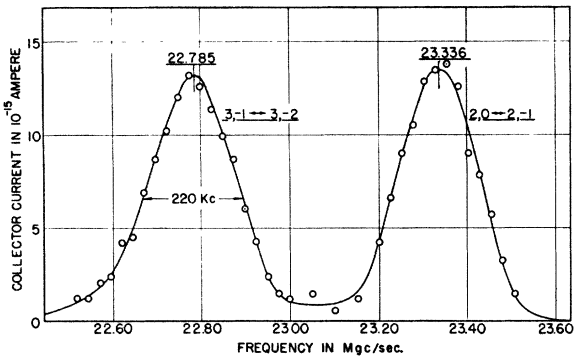

FIG. 4. Resonance curves for the two low frequency resonances, which fulfill the refocusing condition of the present experiment. The widths of the lines are due to inhomogeneity of the steady magnetic field. Similar curves are obtained for Cl^{37}.

far as the above relations are concerned, this is equivalent to a single valence electron in a $^2P_{3/2}$ state, except for a change in the sign of b.[c]

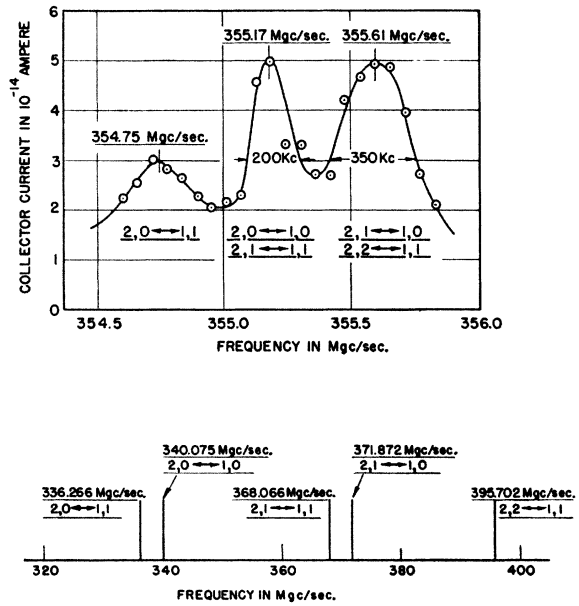

FIG. 5. Upper curve shows resonance curve for Cl^{35} for the transitions between $F=1$ and $F=2$. The five possible transitions are coalesced into three. The intensities can be qualitatively accounted for by considering the transition probabilities of Table I and remembering that in the present experiment the radiofrequency field is predominantly perpendicular to the steady field. The line widths are due to inhomogeneity of the steady field, and to incomplete superposition of adjacent peaks. Lower part of diagram shows positions, frequencies, and quantum number assignments for five of the high frequency transitions of Cl^{35}, in a field strong enough so that all five lines are resolved.

[c] The case of a closed shell minus one electron can be treated by subtracting, from the energy of the closed shell (no h.f.s.), the interaction due to a single electron in a $^2P'_{3/2}$ state, with $\mathbf{S}'=-\mathbf{S}$, $\mathbf{L}'=-\mathbf{L}$, and $\mathbf{J}'=-\mathbf{J}$. Since both magnetic terms in the h.f.s. formula are linear in J', and must be subtracted, there results no change in sign. The quadrupole term, however, is quadratic in J'; hence, subtraction leads to a change of sign.

Alternatively, it is possible to replace the hole in the shell by an electron and a positron both having quantum numbers $\mathbf{S}'$, $\mathbf{L}'$, $\mathbf{J}'$, but with the positron having a *negative* mass. This treatment yields the same results.

Both methods lead to an inversion in the order of the fine structure doublet, as compared to the single electron case.

Combining all factors, we have, for the h.f.s. interaction constants of Cl,

$$ha=-\mu_0^2 g_I \mathfrak{F}\frac{2L(L+1)}{J(J+1)}\langle r^{-3}\rangle_{\mathrm{Av}}, \tag{17}$$

$$hb=-e^2QR\frac{2L}{(2L+3)}\langle r^{-3}\rangle_{\mathrm{Av}}, \tag{18}$$

$$\gamma=(b/a)=\frac{e^2Q}{\mu_0^2 g_I}\frac{R}{\mathfrak{F}}\frac{J(J+1)}{(L+1)(2L+3)}=\frac{3}{8}\frac{e^2Q}{\mu_0^2 g_I}\frac{R}{\mathfrak{F}}. \tag{19}$$

From the definition of the nuclear g-factor,

$$g_I=-(m/M_P)\mu/I,$$

where μ is the nuclear magnetic moment in nuclear magnetons, we have, alternatively,

$$\gamma=-\tfrac{3}{8}(e^2/\mu_0^2)(M_P/m)(I/\mu)(R/\mathfrak{F})Q. \tag{20}$$

In the approximation used above, in which it is valid to separate the radial and angular electron wave functions, the dependence of a and b on r is, in both cases, through the same factor, $\langle r^{-3}\rangle_{\mathrm{Av}}$. Hence, the ratio γ does not involve the radial factor, and the value of Q can be obtained directly from γ and a knowledge of μ. However, if μ is not known, or if it is desired to compute either a or b, it is necessary to be able to obtain $\langle r^{-3}\rangle_{\mathrm{Av}}$ by an independent means. The separation between the two members of the fine structure doublet provides an estimate of $\langle r^{-3}\rangle_{\mathrm{Av}}$. Casimir gives for the doublet separation, δ,

$$h\delta=\mu_0^2 Z_i(2L+1)H\langle r^{-3}\rangle_{\mathrm{Av}}. \tag{21}$$

Here H is still another relativistic correction, and Z_i is slightly (≈ 4 units) less than the nuclear charge. The main difficulty, in using this relationship to estimate $\langle r^{-3}\rangle_{\mathrm{Av}}$, arises from the uncertainty in Z_i.

III. APPARATUS

The apparatus used in this experiment is the same as that described by DNZ with minor modifications. A source of atomic chlorine is needed in place of the oven for alkali beams and it was found possible to use chlorine with the discharge tube previously used by Nagle, Julian, and Zacharias for atomic hydrogen.[14] Their source has not been described elsewhere and a diagram of it is shown in Fig. 2. A glass tube with a narrow slit in one end is placed at a voltage antinode in a microwave resonant cavity so that a glow discharge occurs in the chlorine gas for a centimeter or so directly behind the slit. To maintain the discharge, it was necessary to feed into the resonant cavity about 50 watts of cw radiation at 3000 Mc/sec. Cooling of the outer wall

[14] Nagle, Julian, and Zacharias, Phys. Rev. **72**, 971 (1947).

of the glass tube was adequately provided by an air blast. In this device no metal is in contact with the atomic gases and a good ratio of atoms to molecules is found in the resulting beam, as shown by simple magnetic deflection analysis. The flow of chlorine at a rate of 1 cm^3 at N.T.P. per minute was controlled by a Bourdon-type variable leak.

Beam detection was accomplished by the use of the same tungsten hot wire surface ionization detector used by DNZ. In the present experiment, the accelerating potential was reversed so that negative ions produced at the surface of the wire would pass through the mass spectrometer. The efficiency of the detection of chlorine in this manner was found to be about 10^{-4}, but varied from this and in some cases was less by a factor of 10. In the first attempt to detect a beam of chlorine, the efficiency of formation of negative ions correlated well with the existing data on the work function of tungsten and the electron affinity of atomic chlorine, which gives 10^{-4} as the Boltzmann factor. The experiments reported were done at this efficiency. Subsequent attempts with different tungsten wire gave efficiencies from 100 to 1000 times smaller. Figure 3 shows a curve of intensity *versus* accelerating voltage for chlorine. In the experiments the isotope was selected by adjusting the accelerating voltages.

IV. EXPERIMENTS

A. The Determination of the h.f.s. Constants

The experiments were of the "flop-in" type, used first by Zacharias[15] and described in DNZ. In this type of experiment there is a selection rule in addition to the usual $\Delta F=0, \pm1, \Delta m=0, \pm1$. For detection of the transition, the effective atomic magnetic moment must have reversed directions in the field of the deflecting and refocusing magnets. Assuming that the spins of the Cl nuclei are $\frac{3}{2}$, it may be seen from Fig. 1 that eleven transitions satisfy all these conditions, when the fields in the deflecting and refocusing magnets are sufficiently large so that x is ten or more. Two of these transitions as shown in Fig. 4 have $\Delta F=0, \Delta m=\pm1$ and for them the corresponding frequencies approach zero as the field approaches zero. The remaining transitions are of the $\Delta F=\pm1, \Delta m=0, \pm1$ type. With the fields of the magnets adjusted to refocus atoms which make a transition involving a change in m_J at high fields ($x>10$) of $\pm\frac{1}{2}\leftrightarrow\mp\frac{1}{2}$, the two observable low frequency transitions $(3,-1\leftrightarrow3,-2)$ and $(2,0\leftrightarrow2,-1)$ were easily found for both isotopes. To first-order in H the two transitions have the same frequency.

$$\nu(3,-1\leftrightarrow3,-2)=\frac{g_j\mu_0H}{2h}+\frac{1}{20}\frac{(g_J{}^2\mu_0{}^2H^2)}{ha(1+\gamma/3)}, \quad (22)$$

[15] J. R. Zacharias, Phys. Rev. 71, 909 (1947).

$$\nu(2,0\leftrightarrow2,-1)=\frac{g_J\mu_0H}{2h}+\frac{1}{20}\frac{g_J{}^2\mu_0{}^2H^2}{ha}\times\left\{\frac{2}{(1-\gamma/2)}-\frac{1}{3(1+\gamma/3)}\right\}. \quad (23)$$

The second-order terms indicate that the $(2,0\leftrightarrow2,-1)$ transition will have the higher frequency, provided γ is sufficiently small.

Most of the high frequency transitions, observable with the above refocusing condition, occur between the states $F=2$ and $F=1$. The corresponding transition frequencies will be found near the value $2a-b$ for small x. An estimate of the $F=2\leftrightarrow F=1$ transition

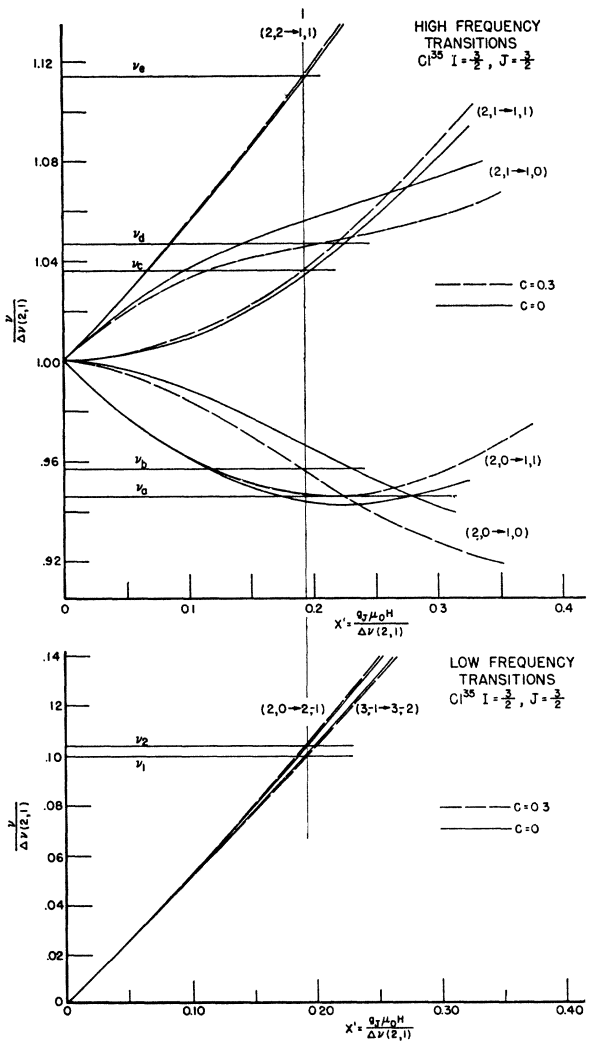

FIG. 6. Plot of the transition frequencies in terms of $\Delta\nu(2,1)=2a-b$ for the seven transitions between states $F=1$ and $F=2$ subject to the refocusing condition that m_J change from $\pm\frac{1}{2}$ to $\mp\frac{1}{2}$. The solid curves are plotted for b/a assumed zero and the dashed curves for $b/a=0.3$. The horizontal lines are drawn in at ordinate values corresponding to observed transitions. They should intersect the theoretical curves for one pair of values of x' and b/a.

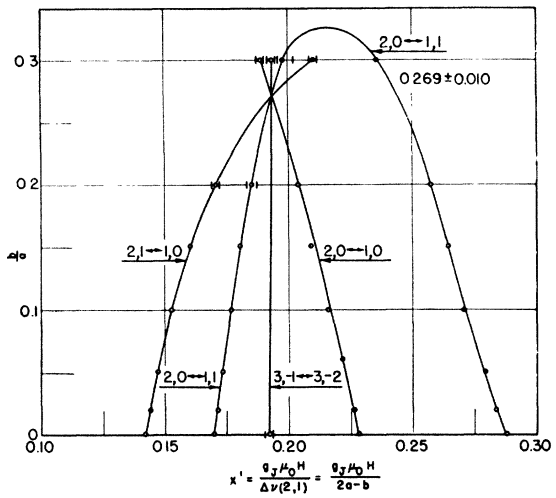

FIG. 7. Plot of b/a against x' for four of the experimental data. Each experimentally observed frequency is used to determine pairs of values of b/a and x', in the neighborhood of values expected to give a consistent set for all four. The common point of intersection of all four curves yields a value of b/a, which is substituted in the secular determinant.

frequency was made by assuming $b/(2a-b)$ to be negligible and solving for $(2a-b)$ in the above two relations for low frequency transitions observed at the same (small) x. In this manner a first estimate of 340 Mc/sec. was obtained for the frequency corresponding to $(2a-b)$. A search near this frequency value in weak fields revealed five resonances.

Again the identification of the transitions depends upon the assumed value of γ. As the field is reduced, the two highest frequency lines which are field dependent become unresolved. The next two lines also merge into one, but are field independent. The lower frequency line is field dependent, increasing in frequency as the field is decreased. Assuming γ to be small, the following identification is tentatively made. In order of increasing frequency,

$$a=(2,\,0\leftrightarrow 1,\,1),\quad d=(2,\,1\leftrightarrow 1,\,0),$$
$$b=(2,\,0\leftrightarrow 1,\,0),\quad e=(2,\,2\leftrightarrow 1,\,1).$$
$$c=(2,\,1\leftrightarrow 1,\,1),$$

Figure 5 shows curves of the unresolved lines at a low field and the relative positions of the lines at a greater field strength.

Attempting to obtain a value of γ from the analysis of these data, using second-order perturbation theory, does not result in a consistent value. It was found that when the value of the homogeneous field was sufficiently low, so as to make second-order theory applicable, the large line width made the accuracy of the measurements insufficient to determine γ. A numerical solution of the secular determinant for the energy levels was then made for several values of x and γ. With these, a graphical analysis was made on a set of data taken at a field high enough to permit accurate frequency measurements. Figure 6 is a plot of the theoretical transition frequency *vs.* $x'=g_i\mu_0 H/(2a-b)$ for two assumed values of γ for the five transitions of interest. The observed transition frequencies, in the same magnetic field, are shown as horizontal lines, from which it is easily seen that the value $\gamma=0$ does not correlate with the observed frequencies for any given value of x', while $\gamma=0.3$, $x'\cong 0.19$ would be consistent with the data. When the same data, and curves for several values of γ are plotted with expanded scales, the appropriate values of x' and γ can easily be determined. Figure 7 is a plot of the values of γ which yield the observed frequencies, against the field parameter x'. The only consistent values are $\gamma=0.269\pm 0.010$ and $x'=0.196$.

From this preliminary determination of γ and the value of $2a-b$, the other two zero field h.f.s. separations may be calculated and search for them can be undertaken. With the same refocusing condition, $m_J=\pm\frac{1}{2}\leftrightarrow\mp\frac{1}{2}$, the only observable transition between $F=3$ and $F=2$ is $(3,\,-1\leftrightarrow 2,\,-1)$. A resonance was found at 671.208 Mc/sec. which was field independent and could be ascribed to the $(3,\,-1\leftrightarrow 2,\,-1)$ transition.

There are no transitions between the states $F=1$ and $F=0$ involving a change in the sign of the effective atomic magnetic moment at high fields. However, the effect of a non-refocusing transition was observed by establishing a competition which involved atoms in one of the states for which a transition can be observed. The apparatus was adjusted so that a transition was being observed between the states $F=1$ and $F=2$, say $(2,\,1\leftrightarrow 1,\,0)$. If now a second r-f field is superposed at a frequency which corresponds to the transition $(1,\,0\leftrightarrow 0,\,0)$, there will exist a competition for atoms which are in the state, $F,\,m=1,\,0$. Those atoms which make the transition $(1,\,0\rightarrow 0,\,0)$ will be, in the high field of the second deflecting magnet, in a state of $m_J=-\frac{3}{2}$ and thus will be deflected past the detector ribbon. The observed $(2,\,1\leftrightarrow 1,\,0)$ transition intensity will therefore decrease. Such an effect was observed; with a $(2,\,1\leftrightarrow 1,\,0)$ intensity corresponding to a 300-mm

TABLE II. Frequencies of various transitions observed in weak magnetic field.

	Cl^{35}			Cl^{37}		
Transition used	$(1,\,0\rightarrow 0,\,0)$	$(2,\,0\leftrightarrow 1,\,0)$	$(3,\,-1\leftrightarrow 2,\,-1)$	$(1,\,0\rightarrow 0,\,0)$	$(2,\,0\leftrightarrow 1,\,0)$	$(3,\,-1\leftrightarrow 2,\,-1)$
Observed frequency	150.020 mc	355.229	671.208	127.477 mc	298.116	555.310
$\Delta F=0$ transition frequency $(3,\,-1\leftrightarrow 3,\,-2)$	0.510 mc	0.500	1.500 mc	0.499	0.516	1.500
Corrected frequency $(x=0)$	149.996 mc	355.230 mc	671.212	127.428	298.117	555.317 mc
Theoretical splitting $(x=0)$	$a-b$	$2a-b$	$3a+b$	$a-b$	$2a-b$	$3a+b$

TABLE III. Values of nuclear electric quadrupole moments.

Nucleus	γ	μ	I	$\mathcal{F}/R$	$Q\times10^{24}$ cm^2
$_{13}Al^{27}$	0.198	3.6419	5/2	0.99640	0.156
$_{17}Cl^{35}$	0.26961	0.8222	3/2	0.99385	−0.0795
$_{17}Cl^{37}$	0.25342	0.683	3/2	0.99385	−0.0621
$_{31}Ga^{69}$	0.32768	2.001	3/2	0.97960	0.2318
$_{31}Ga^{71}$	0.16252	2.543	3/2	0.97960	0.1461
$_{49}In^{115}$	1.85599	5.502	9/2	0.94930	1.166

galvanometer deflection, a decrease of 30 mm was observed when the frequency corresponding to the $(1, 0\rightarrow0, 0)$ transition was applied.

Precise values of the h.f.s. separation frequencies were obtained by observing a high frequency transition, for which $F=\pm1$, and a low frequency transition for which $F=0$, both in the same very small field. The $F=0$ transition frequency and the approximate values of a and b were used to obtain the value of the field parameter, x, which was then used in the expressions obtained by second-order perturbation theory to correct the measured frequency of the $F=\pm1$ transition to its value at zero field. Table II contains the results for both isotopes.

B. Sign of the Magnetic Moment

As described in the previous paper, a change in the sign of the nuclear magnetic moment alters the energy level diagram, shown in Fig. 1, in three ways: (1) The diagram will invert; for a positive moment, which corresponds to positive a, the largest F value has the highest energy, while for a negative moment, the lowest F value has the highest energy. (2) The inversion of the diagram, with change of sign of the nuclear moment, is accompanied by a change of the signs of the low field quantum number m and the high field quantum numbers m_I and m_J. Thus the curve in Fig. 1 which corresponds to $F=1$, $m=-1$, and $m_I=\frac{1}{2}$, $m_J=-\frac{3}{2}$ for positive a, becomes $F=1$, $m=1$, $m_I=-\frac{1}{2}$, $m_J=\frac{3}{2}$ for a negative moment. (3) Change of sign produces a slight change in the energy level values, as described in DNZ.

A particular observable transition frequency will, therefore, involve states whose quantum numbers depend upon the sign of the nuclear magnetic moment. Since the direction of the forces on the atoms in an inhomogeneous magnetic field depends upon the sign of m_J, the trajectory for a given transition will depend upon the sign of the nuclear moment.

A transition frequency was chosen which corresponds to a change in m_J from $+\frac{1}{2}$ to $-\frac{3}{2}$, if μ_n is positive, and from $-\frac{1}{2}$ to $+\frac{3}{2}$ if μ_n is negative. To observe this transition, the field in the refocusing magnet must be lowered by a factor of three, to refocus the $m_J=\pm\frac{3}{2}$ states. A determination of which of the two possible trajectories is the one involved in the transition is made by observing the transition intensity as the obstacle wire is moved to obstruct one of the possible paths.

The experiment was done with Cl^{35} by observing the transition characterized by $(2, 0, -\frac{1}{2}, \frac{1}{2}\rightarrow1, -1, \frac{1}{2}, -\frac{3}{2})$ for nuclear moment assumed positive or characterized by $(2, 0, \frac{1}{2}, -\frac{1}{2}\rightarrow1, 1, -\frac{1}{2}, \frac{3}{2})$ for nuclear moment assumed negative. The intensity corresponding to this transition was found to disappear when the wire was moved in the direction of decreasing field. Therefore, it can be concluded that the sign of the Cl^{35} nuclear moment is positive. The experiment was not repeated for Cl^{37}, but it is assumed that the signs of the magnetic moments are alike for the two isotopes, since the magnitudes of the spin, magnetic, and quadrupole moments are so similar.

V. RESULTS AND DISCUSSION

A. The Nuclear Spin

One result of the experiments described above is to confirm the assignment of the spin value $\frac{3}{2}$ for both chlorine isotopes. The spin value is arrived at by two independent sets of observations: (1) The observed h.f.s. pattern is consistent with no other value of the nuclear spin than $I=\frac{3}{2}$ and no other value of the electronic angular momentum than $J=\frac{3}{2}$. Any other values would lead to a completely different set of observable transitions, and a completely different dependence of the frequencies of these transitions on the strength of the applied magnetic field. (2) Observations of the slope of the curve of frequency *vs.* applied field, for the low frequency transitions in weak magnetic field, are consistent only with $I=\frac{3}{2}$, assuming a $^2P_{3/2}$ electronic configuration. The use of this method for nuclear spin determination has been described in the preceding paper.

TABLE IV. Effective nuclear charge, Z_i, as computed from the magnetic h.f.s. splitting and the fine structure.

Isotope	Z	I	State	a(Mc/sec.)	$\delta(10^4$ Mc/sec.)	$\mathcal{F}/H$	Z_i	$Z-Z_i$
Al^{27}	13	5/2	$^2P_{1/2}$	488.0	335.78	1.0127	9.85	3.15
			$^2P_{3/2}$	94.27		0.9996	10.04	2.96
Cl^{35}	17	3/2	$^2P_{3/2}$	205.288	2641.0	0.9993	13.64	3.36
Cl^{37}	17	3/2	$^2P_{3/2}$	170.686		0.9993	13.63	3.37
Ga^{69}	31	3/2	$^2P_{1/2}$	1338.78	2476.1	1.0770	25.72	5.28
			$^2P_{3/2}$	190.790		0.9974	33.43	−2.43
Ga^{71}	31	3/2	$^2P_{1/2}$	1701.05	2476.1	1.0770	25.73	5.27
			$^2P_{3/2}$	242.424		0.9974	33.44	−2.44
In^{115}	49	9/2	$^2P_{1/2}$	5706.5	6632.8	1.2175	41.87	7.13
			$^2P_{3/2}$	242.156		0.9925	64.35	−15.35

TABLE V. Ratio of magnetic h.f.s. interactions.

Isotope	$a(1/2)/a(3/2)$ uncorrected	$\mathfrak{F}(1/2)$	$\mathfrak{F}(3/2)$	$a(1/2)/a(3/2)$ corrected
Al^{27}	5.17	1.017	1.004	5.10
$Ga^{69,71}$	7.02	1.102	1.020	6.50
In^{115}	9.43	1.291	1.052	7.68

B. The h.f.s. Interaction Constants

The data of Table II lead to the following values of the interaction constants

$$a_{35}=205.288\pm0.010 \text{ Mc/sec.},$$
$$b_{35}=55.347\pm0.020 \text{ Mc/sec.},$$
$$\gamma_{35}=(b/a)_{35}=0.26961\pm0.00010,$$
$$a_{37}=170.686\pm0.010 \text{ Mc/sec.},$$
$$b_{37}=43.256\pm0.020 \text{ Mc/sec.},$$
$$\gamma_{37}=(b/a)_{37}=0.25342\pm0.00010.$$

The measurements yield three independent frequencies between the 4 h.f.s. levels, but there are only two independent constants involved. The fact that all the data are consistent with the above constants, to within the experimental accuracy, provides an excellent check for the theory of the atomic hyperfine structure and its Zeeman effect, and indicates that we have not left out of consideration any significant interactions.

In addition, this consistency enables us to set an upper limit for the nuclear magnetic octupole interaction. An expression for the nuclear magnetic octupole term in the atomic h.f.s.[d] has been derived by Kramers and by Casimir and Karreman,[16]

$$E_{\text{oct}}=hc\{C^3+4C^2+\tfrac{4}{5}C[-3J(J+1)I(I+1)+J(J+1)+I(I+1)+3]+4I(I+1)J(J+1)\}. \quad (24)$$

For $I=J=\frac{3}{2}$, this becomes

$$E_{\text{oct}}=hc\left[C^3+4C^2-\frac{507}{20}C+\frac{225}{4}\right]. \quad (25)$$

TABLE VI. Comparison of atomic and molecular nuclear electric quadrupole interaction constants.*

Nucleus	Molecule	$-eQ[(\partial^2V)/\partial Z^2]$ in Mc/sec.
Cl^{35}	atom	110.694
	ClCN	83.2
	ICl	82.5
	CH_3Cl	75.13
	SiH_3Cl	40.0
Cl^{37}	atom	86.512
	ClCN	65.9
	CH_3Cl	59.03
	SiH_3Cl	30.8

* These values are taken from B. T. Feld, Preliminary Report No. 2, Nuclear Science Series, Nat. Res. Council (1948). The references to the original work may be found in that report.

[d] We are indebted to Dr. W. A. Nierenberg for helpful discussions concerning the correct form of the octupole term.

[16] H. A. Kramers, Proc. Roy. Acad. Amsterdam **34**, 965 (1931); H. B. G. Casimir and G. Karreman, Physica **9**, 494 (1942).

If this term is added to the expression for the interaction energy, the three measured frequencies can then be solved for the three unknowns, a, b, and c. Within the accuracy of the experimental results, $c=0\pm1$ kc/sec.

C. The Nuclear Electric Quadrupole Moments

From the expressions given in Section B, the nuclear electric quadrupole moment of Cl is

$$Q=-(8/3)(\mu_0^2/e^2)(m/M_P)(\mu/I)(\mathfrak{F}/R)(b/a), \quad (26)$$

$$Q=-0.54137(\mu/I)(\mathfrak{F}/R)(b/a)\times10^{-24} \text{ cm}^2. \quad (27)$$

For chlorine, $\mathfrak{F}/R=0.99385$; together with our values for a and b and the values of Taub and Kusch[4] for μ_{35}, we get

$$Q_{35}=(-0.0795\pm0.0005)\times10^{-24} \text{ cm}^2,$$
$$Q_{37}=(-0.0621\pm0.0005)\times10^{-24} \text{ cm}^2.$$

The negative sign follows from the observation that (b/a) is positive and that μ is positive, in agreement with the independent determination of the sign of μ by Kusch and Millman.[2] The accuracy of the above values of Q is limited only by the accuracy in the knowledge of μ, and in the calculation of the relativistic corrections.

The method used by us to evaluate Q is much more accurate than the one involving the fine structure splitting. As far as we know, it has not been previously used, even in the cases where a, b, and μ were known with sufficient accuracy. We have therefore re-evaluated the results of the previous measurements, and obtained more accurate values of the nuclear electric quadrupole moments as shown in Table III. The Ga data are from the paper of Becker and Kusch.[9] The values for In^{115} were given by Mann and Kusch.[17] The nuclear moments are taken from the Table III of Taub and Kusch.[4]

D. Atomic Properties from the h.f.s.

As previously noted, the usual procedure for evaluating the nuclear electric quadrupole moment, from the observed h.f.s. interaction, involves the use of the atomic fine structure splitting, δ, in order to eliminate the factor $\langle r^{-3}\rangle_{\text{Av}}$. This method requires estimating the factor Z_i the effective nuclear charge, which is usually taken to be $Z-4$. We have eliminated this uncertainty, by the method discussed in the preceding sections.

However, it should be possible to reverse the usual procedure, and to obtain an estimate of Z_i from the observed h.f.s. and fine structure splitting, by comparing the magnetic dipole interactions in the two cases. Application of the formulas yields

$$Z_i=(\mu/I)(m/M)(\mathfrak{F}/H)\frac{2L(L+1)}{(2L+1)J(J+1)}\left(\frac{\delta}{a}\right). \quad (28)$$

The values of Z_i, computed from this formula on the

[17] A. K. Mann and P. Kusch, Phys. Rev. **76**, 163 (1949).

basis of the constants previously discussed, are given in Table IV. Whenever available, the h.f.s. interactions in the $^2P_{1/2}$ state have been used as well as those for the $^2P_{3/2}$ state.

The most striking aspect of Table IV is the serious failure to obtain agreement, for the heavy elements, between the two values of Z_i calculated, from the constants for the two atomic states. Indeed, for Ga and In the values of Z_i, derived from the $^2P_{3/2}$ data, are actually larger than the nuclear charge, Z. This discrepancy is very serious, and casts considerable doubt on the adequacy of the theory, in the case of heavy elements.

The failure of the theory for heavy elements is probably associated with its breakdown at distances close to the nucleus. The value of $\langle r^{-3}\rangle_{Av}$ is strongly dependent on the shape of the wave function close to the nucleus, as is the quantity $\langle(1/r)(\partial V/\partial r)\rangle_{Av}$, which appears in the expression for δ, and which is approximated by $Z_i\langle r^{-3}\rangle_{Av}$.

The departures of the theory from the simple form, applicable for light elements, is presumably taken into account by the relativistic corrections. For Ga and In the individual corrections become quite large, although the ratios which appear in some of our expressions, may be fortuitously small. Thus, for instance, the correction, $\mathfrak{F}$, for the nuclear magnetic dipole interaction constant, is 1.102 for Ga and 1.291 for In, in the $^2P_{1/2}$ states. The large size of these corrections is another manifestation of difficulties with the simple theory at distances close to heavy nuclei.

The conclusion to be drawn from the failure of the theory is that the radial dependence of the wave function, in the vicinity of the nucleus, is different for the $J=\frac{3}{2}$ and the $J=\frac{1}{2}$ states. This is illustrated by a comparison of the magnetic dipole h.f.s. terms, for the same nucleus, corresponding to these states. The simple theory gives

$$[(a/\mathfrak{F})^2P_{1/2}/(a/\mathfrak{F})^2P_{3/2}]=5.$$

Table V gives the experimental values of the above ratio, uncorrected for relativistic effects (column 2), and corrected (last column). For the heavy nuclei, the ratio deviates considerably from the value 5.

It should be pointed out that, despite the discrepancies discussed above, the values of the nuclear electric quadrupole moments, computed by our method and given in Table III, do not suffer from these difficulties. Our method takes advantage of the fact that, whatever the shape of the electronic wave function, the dependence on the wave function is the same for both the magnetic dipole and electric quadrupole terms, and can therefore be eliminated, provided only that the radial and angular dependence are separable.

While there seems no reason to believe that the failure of the theory is associated with any inadequacy of the Russel-Saunders coupling approximation, these results indicate that L-S coupling requires more careful investigation, in the case of heavy nuclei.

E. Molecular Properties from the h.f.s.

As mentioned in the introduction to this paper, C. H. Townes has proposed a method for computing the nuclear electric quadrupole interaction in certain molecules. The nuclear electric quadrupole moments of the chlorine isotopes, as estimated by Townes, are in reasonable agreement with the values obtained by us.

However, once the nuclear electric quadrupole moment is known, the molecular h.f.s. constant can be used to obtain information concerning the molecular properties. In particular, for a molecule in which the Cl atom is predominantly covalently bonded, the deviation of the observed quadrupole interaction constant, $eQ(\partial^2V/\partial Z^2)$, from that predicted from the atomic case can be used to draw conclusions regarding the amount of non-covalent bonding, the $s-p$ hybridization, and other important molecular properties.

Table VI compares the quadrupole interaction constants of atomic Cl and a number of symmetric rotor molecules. The atomic constant, which corresponds to the molecular $eQ(\partial^2V/\partial Z^2)$ is, in this case, $-2b$; the factor, -2, arises from the fact that the molecular quadrupole interaction constant is defined as the average about the axis of molecular symmetry.

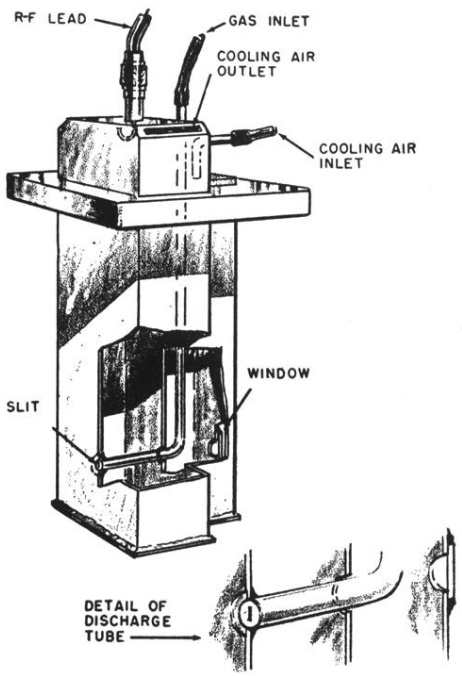

FIG. 2. Cut-away sketch of resonant cavity and gas system for producing atomic chlorine from Cl_2.